ISSN: 0067-2904

Influence of Fe_2O_3 Dust Particles on the Plasma Characteristics of D.C Sputtering System

Shahad Emaduldeen Abdulghani*, Qusay A. Abbas
Physics department, College of Science, University of Baghdad, Baghdad, Iraq

Received: 13/11/2021 Accepted: 10/3/2022 Published: 30/7/2022

Abstract

This work is an experimental study conducted to study the effects of iron oxide dust particles (Fe_2O_3) on the characteristics of DC discharge plasma in argon gas under vacuum. Electron temperature (T_e) and electron density (n_e) were calculated by Boltzmann plots and Stark broadening, respectively. The results show that both the electron density and plasma frequency (ω_{pe}) increased with the operating pressure. While, T_e and Debye length (λ_D) decreased with pressure. The glow discharge is more stable with the Fe_2O_3-dust particles; all dust plasma parameters have lower values than those of the dust-free plasma.

Keywords: Dust plasma, Optical emission spectroscopy, electron temperature, electron density. Plasma parameters

تأثير غبار جسيمات Fe_2O_3 على خصائص البلازما في منظومة ترسيب التيار المستمر

شهد عماد الدين عبد الغني*، قصي عدنان عباس
قسم الفيزياء , كلية العلوم, جامعة بغداد, بغداد, العراق

الخلاصة

هذا العمل عبارة عن بحث تجريبي أجري حول تأثير غبار دقائق اوكسيد الحديد (Fe_2O_3) على خصائص بلازما تفريغ التيار المستمر في الأرجون تحت التفريغ .تم حساب درجة حرارة البلازما (T_e) و كثافة الإلكترونات (n_e) بواسطة طريقة بولتزمان وطريقة ستارك لتوسع الخطوط الطيفية ، على التوالي. أظهرت المعلمات المقاسة أن كلا من كثافة الإلكترون وتردد البلازما (ω_{pe}) يزداد مع زيادة ضغط الغاز. بينما انخفضت درجة حرارة الإلكترون وطول ديباي (λ_D) مع زيادة ضغط الغاز. تكون البلازما أكثر ثباتًا مع غبار جزيئات Fe_2O_3 ، وكل معاملات البلازما لها قيم أقل في حالة وجود غبار Fe_2O_3 مقارنة بالبلازما الخالية من الغبار.

1. Introduction

Plasma containing suspended charged particles of micron or nanometer size (in addition to electrons, ions and neutral atoms) is called dusty plasma or complex plasma. Dusty plasma is usually a low-temperature plasma in which the gas is partially ionized and contains relatively large suspended particles compared with electron or positive ions. [1]. It has the ability to self-regulate. It has gained much interest in recent research. The presence of these large

*Email: Shahademaduldeen@gmail.com

charged particles considerably changes the equilibrium of charge within the plasma, causing distinctive features. The essential characteristic that distinguishes dusty plasma is the mutual interaction between charged dust particles, which leads to their growth inside the plasma to form larger grains, which results in the granular plasma and the formation of structures arranged with crystal structures [2].

The micro-particles become the dominant class of plasma so that they can be considered a single-species system, where the greatest influence on the properties of the plasma is the energy or momentum of these particles. The crystallization, wave and defect propagation can be studied for dust plasma [3].

since electrons have higher mobility than ions, this leads to a negative dust charge. A micrometer-sized dust particle can have a negative charge of thousands of electron charges. This means that the dust is trapped by the electric field inside the plasma due to its large surface negative charge which represents the bulk of the plasma [4]. Grain dust particles can be grown by sputtered particles or reactive gasses [5].

Dusty plasma is abundant in many phenomena, as it is considered a component of the Earth's magnetosphere and the cosmic plasma in comets or the heliosphere and others. [6]. In addition, it consists in laboratory plasma, plasma applied in industrial material for microelectronic processing and plasma in fusion devices [7]. The prevalence of dusty plasma systems, their ease of generation, their special diagnostic methods [8] and control of its parameters [9], and many unique transport features make the dust plasma a subject of much research, which are not only for general physical but also a technological benefit. Different methods are used to produce dust plasma under laboratory conditions [10].

In many important industrial processes, such as chip production or in plasma fusion, sputter deposition of complex materials dust particles are produced within plasma reactors, the effect of these dust on plasma must be known, hence on its effectiveness [3].

Knowing plasma properties is vital for understanding the techniques by which its properties can be controlled, which are essential in the different applications in which this plasma is involved. Plasma can be diagnosed by electrical probes or optical emission spectroscopy. Plasma spectroscopic diagnosis is one of the most important diagnostic techniques, which gives important information about the state of the plasma; it is a simple technique in addition to its lack of impact on the plasma due to the immersion of probes inside it [11].

α-Fe_2O_3 is a promising magnetic material due its many technical applications. It exhibits a nonlinear relationship between applied magnetic field. It is employed in different uses as a magnetic substance. Furthermore, it used in other devices such as in photovoltaic application [12].

Samsonov et al. [13] studied the aggregation of magnetic particles in dust plasma with the existence of magnetic attraction between particles. Particle analysis showed the interaction between the particles; agglomeration can occur if the energy of the particles exceeds the potential barrier. Rosenberg et al.[14] studied the possibility of using dusty plasma for surface-enhanced vibrational spectroscopy. They found that the plasma reduced aggregation. This allows the use of many dust substances which have resonances in the IR or visible. Jabur et al. [15] the sample of O_2/Ar gaseous mixture by plasma-based DC magnetron sputtering with niobium metal as a target material Plasma diagnosis via the Optical Emission Spectroscopy (OES) method was used to achieve Te and Ne mixture values of 20 %, 30 %, 50%, and 70% in the Ar/O_2 system. Hameed and Kadhem [16] constructed a gliding arc discharge (GAD) with a water spray system. A non-thermal plasma generated between two V shaped electrodes in an ambient argon driven by 100 Hz AC voltage with different gas flow rates (0.5, 1, 1.5, 2 , 2.5 , 3 1/min)was investigated using optical emission spectroscopy (OES).

2. Theoretical part

In order to determine the plasma parameters, such as plasma temperature (T_e), electron density (n_e), Debye length (λ_D), and plasma frequency (ω_{pe}), optical emission spectroscopy was used. Boltzmann distribution is fulfilled in situations of local thermodynamic equilibrium [17]. The Boltzmann plot method is widely used for spectroscopic measurements and for the determination of T_e [18]:

$$Ln\left(\frac{I_{ji}\lambda_{ji}}{h\ c\ g_j A_{ji}}\right) = \left(-\frac{E_j}{k_B T_e}\right) + Constant \quad (1)$$

Where: I_{ji}, is the intensity, A_{ji} is the probability of transition, g_j is a statistical weight of upper levels of the selected lines, h is Planck's constant, λ_{ji} is the wavelength corresponding to the transmission down from upper level j to lower level i for the same species in the same ionization degree.

The Stark broadening effect was used to calculate n_e according to the line broadening $\Delta\lambda$ [19]:

$$n_e(cm^{-3}) = \left[\frac{\Delta\lambda}{2\omega_s}\right] N_r \quad (2)$$

Where: ω_s is the electron-impact value and Nr is the reference density which equals $10^{16} cm^{-3}$ for atomic lines and $10^{17} cm^{-3}$ for singly ionized ions lines.

Plasma frequency can be given as [20]:

$$\omega_{pe} = \sqrt{\frac{n_e\ e^2}{m_e\ \varepsilon_0}} \quad (3)$$

Where $\varepsilon_0$is the free space permittivity, m_e is the electron mass.

Debye's length can be calculated by the formula [20]:

$$\lambda_D = \sqrt{\frac{\varepsilon_0\ k_B\ T_e}{e^2\ n_e}} \cong 743 \sqrt{\frac{T_e\ (eV)}{n_e\ (cm^{-3})}} \quad (4)$$

Where: k_B is Boltzmann's constant.

In this study, the influence of Fe_2O_3 powder, dusted within plasma, on its characteristics and on plasma parameter, in dc discharges of argon, were studied at different vacuum pressures.

3. Experimental setup

A schematic diagram of the dust plasma DC discharge system is shown in Figure 1. It consists of two parallel aluminum plane electrodes of 6cm in diameter. Both electrodes were fixed and isolated by Teflon caps to prevent any sparks with the chamber walls. Two concentric circular magnets behind the cathode were utilised as a magnetron to confine the plasma.

The discharge system was operated in DC mode across a high purity argon gas under vacuum. Normal glow discharge was produced using 10kV DC across the electrodes, and then the voltage of the electrodes was dropped. The system was operated under different pressures from 0.06 to 0.4 Torr

Micrometer sized Fe_2O_3 particles with a weight of 100 g were dusted between the electrodes inside the chamber by a duster device; the dust cloud could be observed by the naked eye. The fall-down particles on the electrodes were removed after each experiment.

Spectroscopic analysis of the emitted plasma was done using an optical emission spectrometer.

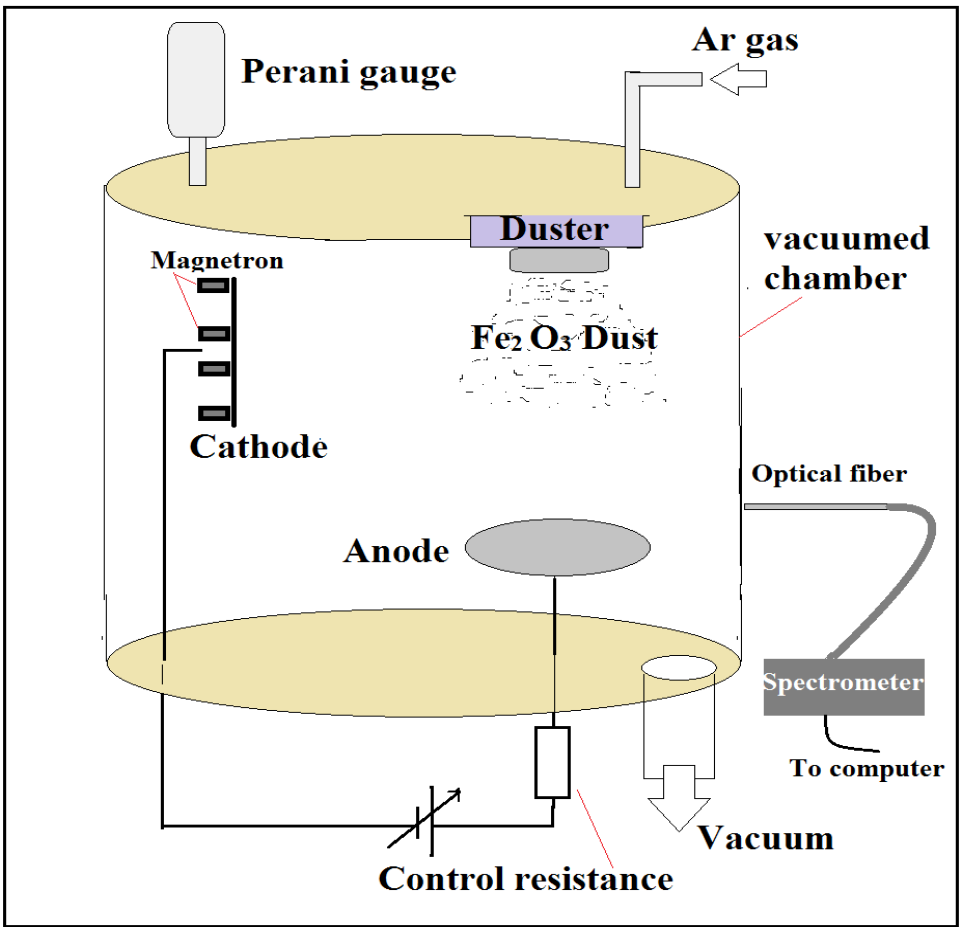

Figure 1-Schematic diagram of the dust plasma DC discharge system.

4. Results and Discussions

Ar plasma emission spectra of the DC discharge system at different gas pressures (0.06, 0.08, 0.2 and 0.4 Torr) with and without Fe_2O_3 dust particles are shown in Figure 2 A and B. The figure shows many atomic and ionic argon emission lines (Arl and ArII) of different intensity peaks according to their probability of the corresponding transition, the statistical weight of the upper levels, and plasma temperature. The additional peak corresponding to Hα electronic transmission at 656.7 nm comes from the residual light hydrogen atoms due to the chamber evacuation.

All peaks intensity increased with increasing the pressure (between 0.6-0.4 Torr) inside the chamber, due to the increase of the excitation collisions probability between electrons and atoms of higher density. While, the presence of dust particles between the electrodes caused a decrease in the peak intensity in the plasma emission spectrum. The mean free path of electrons was reduced as a result of their collisions with the dust particles which reduced their energy, hence reducing the probability of excitation collisions. In addition, dust reduced the emission intensity further due to plasma confinement by the suspended charged particles.

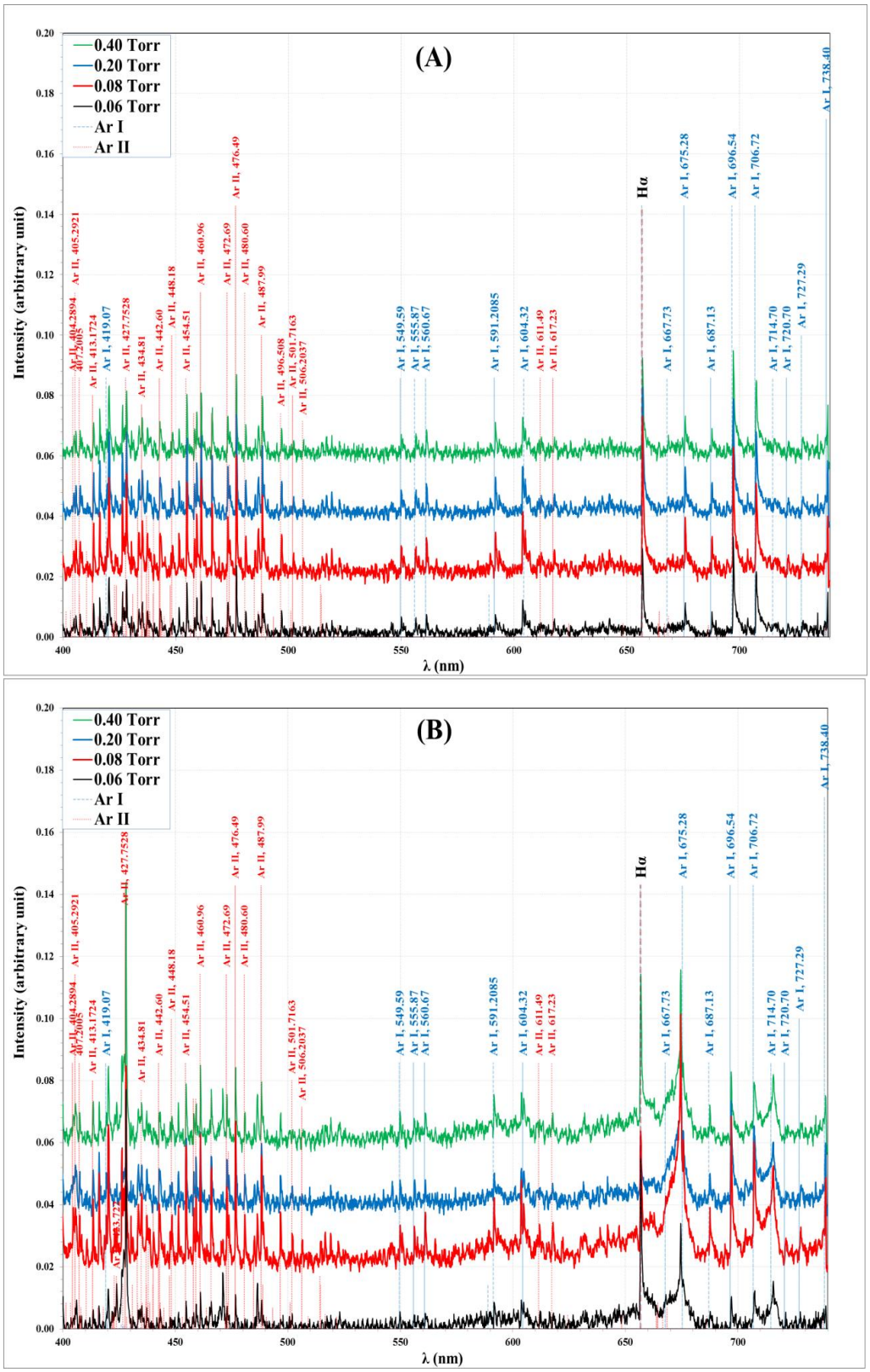

Figure 2-Ar plasma emission spectra at different gas pressure: (A) without and (B) with dust particles.

Electron temperature (T_e) is responsible for various excitation and ionization processes that occur in the plasma, so the lines intensities vary according to the (T_e) as described by Boltzmann plots. In this method, the relation of $Ln(I_{ij}\lambda_{ij}/ hc\ g_j\ A_{ij})$ against the upper-level

energies (E_j) is plotted for parameters of observed lines from the same atomic species. The value of T_e is equal to the reverse of the slope for the best fitting line of this plot. The parameters of the used line are illustrated in Table 1. Figure 3 shows Boltzmann plots employing the selected atomic argon peaks (*ArI*) for the DC discharge system in the two cases of dust-free and with dust under the different gas pressures.

Table 1- Wavelength *λij, Aij.gj*, upper level energy *Ej*, and lower level energy *Ei* for ArI lines

λ_{ij} (nm)	$A_{ij}.g_j$	E_j (eV)	E_i (eV)
550.6113	2.50E+06	13.094873	15.346003
555.8702	7.10E+06	12.907015	15.136848
560.6733	6.60E+06	12.907015	15.117746
591.2085	3.15E+06	12.907015	15.003566
603.2127	2.21E+07	13.075716	15.130544
675.6163	1.80E+06	13.302227	15.136848
687.1289	8.34E+06	12.907015	14.710898
696.5431	1.90E+07	11.548354	13.327857
706.7218	1.90E+07	11.548354	13.302227
714.7042	1.90E+06	11.548354	13.282639
720.6980	7.44E+06	13.302227	15.022088
727.2936	5.49E+06	11.623593	13.327857

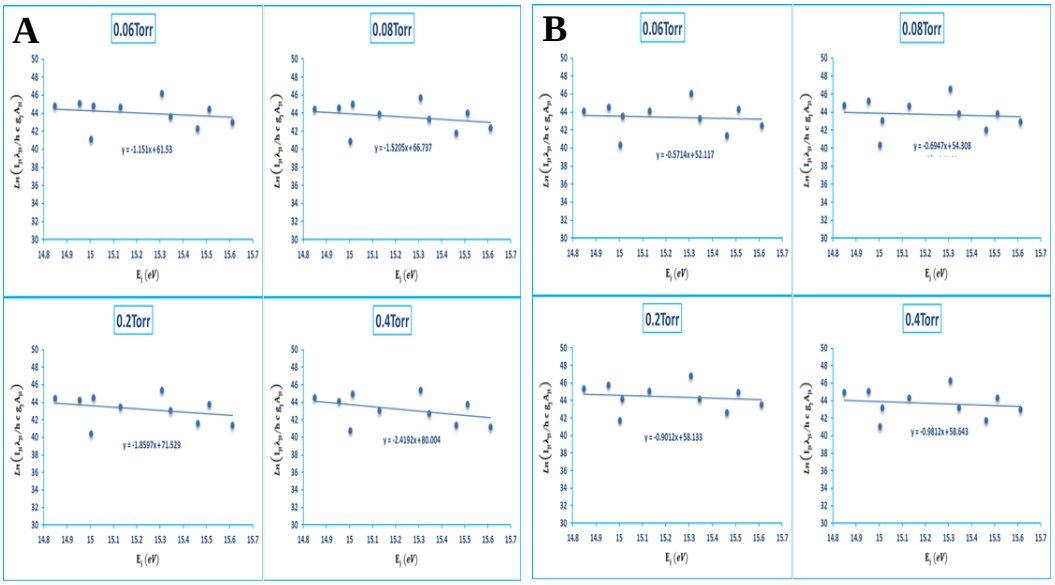

Figure 3- Boltzmann plots for Arl peaks for the DC discharge system at different gas pressures (A) with and (B) without Fe_2O_3 dust particles.

Figure 4 shows the variation of T_e with the operating gas pressures in the two cases: with and without Fe_2O_3 dust particles. The electron temperature decreased with the increase of the pressure for the two cases. The graphs show two regions: a sharp decrease in the electron temperature from 1.8 to 1.4eV for the dust-free plasma and from 0.9 to 0.65 eV for the dust plasma when the pressure increased from 0.06 to 0.08 Torr. The second region, T_e decreased slowly from 1.4 to 1eV for the dust-free plasma and from 0.65 to 0.4eV for the dust plasma as the pressure increased from 0.08 to 0.4 Torr. The decrement in T_e with the increase of the operating pressure is due to the increase of electron-atom inelastic collisions; some of the electron energy is transferred to the gas atoms causing the increase of their energy while the average kinetic energy of the electrons decreases. On the other hand, T_e in the dust plasma is

less than in the dust-free due to the existence of the Fe_2O_3 particles, which alters the charged particle equilibrium that affects the electron energy by complicating the plasma.

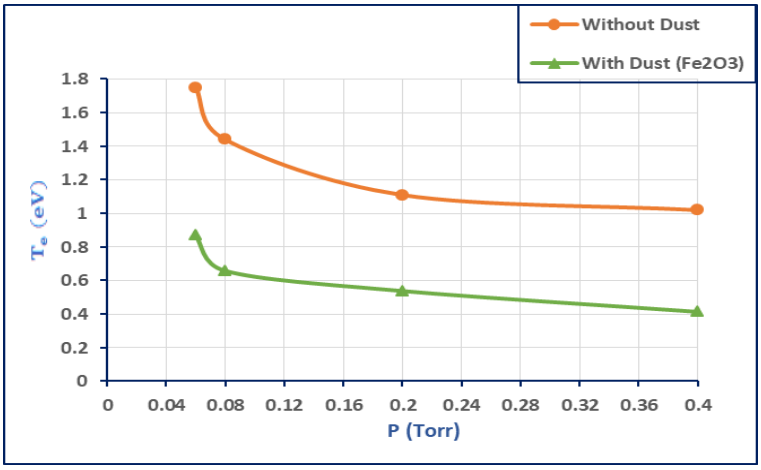

Figure 4- the variation of *Te* against the gas pressure with and without dust.

One of the most common methods for determining electron density (n_e) is Stark's principle of spectral lines broadening. The full-width half-maximum values were employed to calculate the electron density using the standard values of the broadening.

The 476.48 nm wavelength ArII line was used to measure n_e. The line broadening was measured using Lorentzian distribution. The used parameters for this line are according to the review of Konjevic and Wiese [21]. The line broadening was found to be (0.54, 0.64, 0.68, and 0.73) nm for the dust-free plasma, while for dust plasma, it was (0.43, 0.48, 0.51, and 0.58 nm) when the pressure varies as 0.06, 0.08, 0.20 and 0.4 Torr, respectively.

Figure 5 illustrates the effect of the pressure on the electron density for the dust-free and dust plasma. One can observe that the electron number density increases with the rising of argon pressure from --- to---Torr in the two cases. The electron number density increased from 7×10^{16} to 9.5×10^{16} cm^{-3} and from 5.5×10^{16} to 7.5×10^{16} cm^{-3} for the dust-free and dust plasma, respectively. The increase of gas pressure at this range led to increase the electron-atom ionization collisions and hence increasing the electron number density. While, the ionization collisions (which is an electron-atom collision with sufficient energy for ionization) decreased remarkably for the dust plasma at all pressures due to reducing the average kinetic energy of electrons, as shown in the previous section.

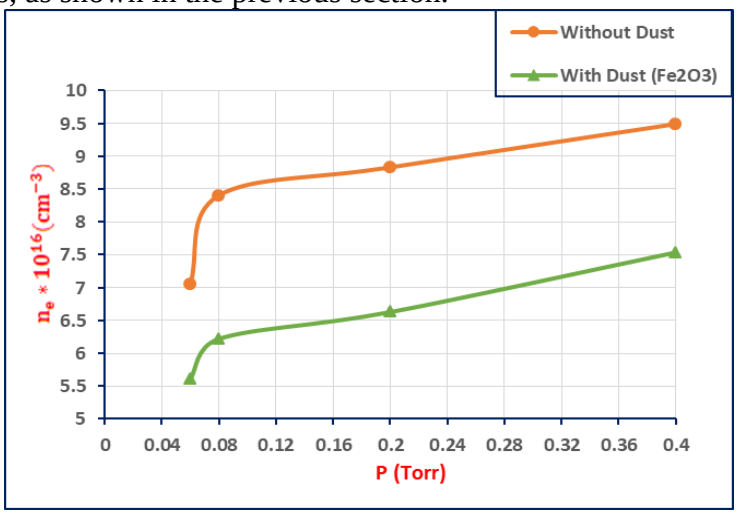

Figure 5- The variation of n_e against the gas pressure with and without Fe_2O_3 dust.

Using Eq. (4), the Debye length (λ_D) was determined. Figure 6 shows the variation of Debye length with the operating pressure for the dust-free and dust plasma. It can be observed that λ_D decreased with increasing the operating pressure in the two cases. Furthermore, the existence of the Fe_2O_3 dust particles caused further reduction in λ_D. These behaviors are due to the increase of electron density with pressure.

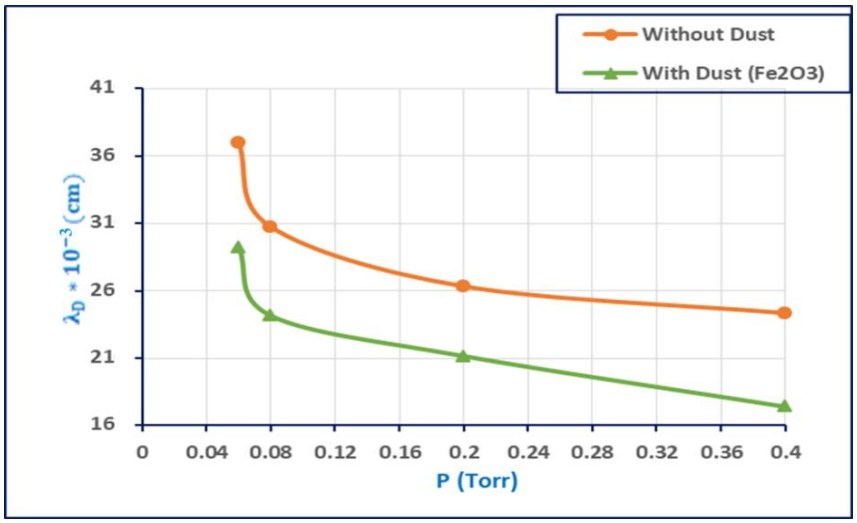

Figure 6-The variation of λ_D against the gas pressure with and without dust.

Figure 7 demonstrated the variation of plasma frequency with the operating pressure in the two cases, with and without Fe_2O_3 dust particles. Plasma frequency increased with increasing gas pressure in both cases with a higher rate in the absence of the Fe_2O_3 dust particles. Without dust, the plasma frequency was increased from 150×10^{11} to 174×10^{11} rad/s. While with Fe_2O_3 dust particles, the plasma frequency increased from 133×10^{11} to 155×10^{11} rad/s. The plasma frequency mainly depends on its electron density, as shown in Eq. (3), so it has nearly the same behavior.

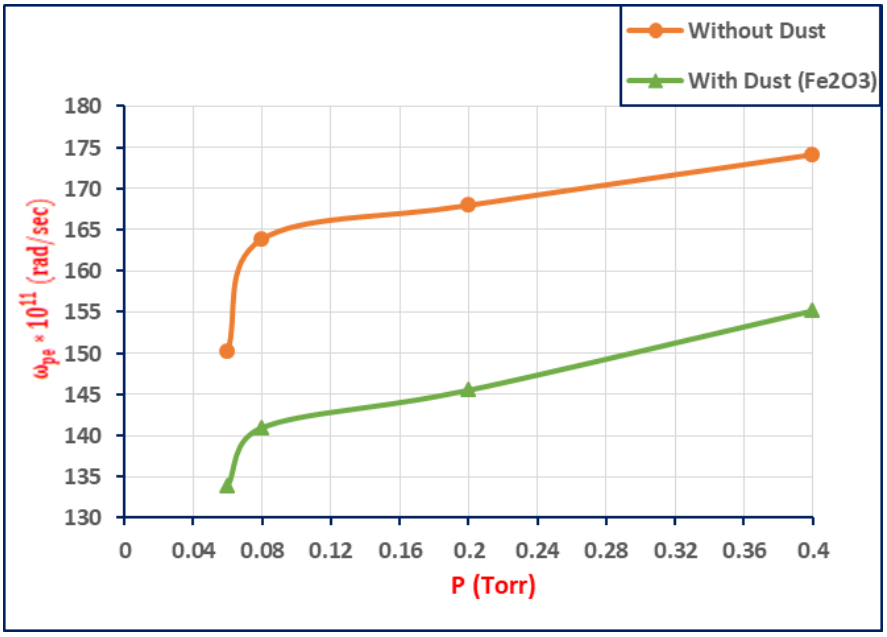

Figure 7- (ω_{pe}) against the gas pressure with and without dust

5. Conclusions

In this work, the effect of Fe_2O_3 dust particles in a DC discharge plasma was studied. Without Fe_2O_3 dust particles, it was observed that the intensity of the emission lines increased with rising the operating gas pressure. Though, with the Fe_2O_3 dust particles, the emission intensity decreased with increasing the operating pressure as a result of the effect of the Fe_2O_3 dust particle, which alter the space charge due to plasma confinement in a region of a strong electric field. In addition, the effect of operating pressure and the presence of Fe_2O_3 dust particles on plasma properties were studied. Electron temperature and Debye length decreased, while the electron density and plasma frequency increased with rising the operating gas pressure. While, the plasma temperature and density were lower with Fe_2O_3 than in the case of dust-free plasma.

References

[1] S. A. Hameed and Q. A. Abbas, "Experimental investigation of dusty plasma characteristics in AC discharge system," *Iraqi J. Phys.*, vol. 13, no. 28, pp. 179–188, 2015

[2] L. G. D'yachkov, O. F. Petrov and V. E. Fortov, "Dusty Plasma Structures in Magnetic DC Discharges," *Contrib. Plasma Phys.*, vol. 49, no. 3, pp. 134 – 147, 2009.

[3] G. E. Morfill and A. V. Ivlev, "Complex plasmas: An interdisciplinary research field," *Reviews of Modern Physics*, vol. 81, no. 4. pp. 1353–1404, 2009.

[4] T. F.Toussaint, "The charge distribution of dust particles in plasma afterglow," *Faculteit Technische Natuurkunde*, 2017.

[5] V. Vekselman, Y. Raitses and M. N. Shneider, "Growth of nanoparticles in dynamic plasma," *Physical Review E*, vol. 99. p. 063205, 2019.

[6] N. Borisov and H. Krüger, "Formation of the Thebe Extension in the Ring System of Jupiter," *J. Geophys. Res. Sp. Phys.*, vol. 126, pp. 1–13, 2021.

[7] M. W. Morooka, J. E. Wahlund, D. J. Andrews, A. M. Persoon, S.Y. Ye, W. S. Kurth, D. A. Gurnett and W. M. Farrell, "The Dusty Plasma Disk Around the Janus/Epimetheus Ring," *J. Geophys. Res. Sp. Phys.*, vol. 123, no. 6, pp. 4668–4678, 2018.

[8] J. G. Choi, H. Y. Kim and H. B. Lim, "Analysis of ferrite powder using inductively coupled plasma atomic emission spectrometry," *Microchem. J.*, vol. 63, no. 1, pp. 119–127, 1999.

[9] R. Merlino, "Dusty plasmas: from Saturn's rings to semiconductor processing devices," *Adv. Phys. X*, vol. 6, no. 1, 2021.

[10] B. Lindstrom, P. Bélanger, A. Gorzawski, J. Kral, A. Lechner, B. Salvachua, R. Schmidt, A. Siemko, M. Vaananen, D. Valuch, C. Wiesner, D. Wollmann, and C. Zamantzas, "Dynamics of the interaction of dust particles with the LHC beam," *Phys. Rev. Accel. Beams*, vol. 23, no. 12, p. 124501, 2020.

[11] M. Zhukov, "*Plasma Diagnostics*," Mosco: Lightning Source UK Ltd., vol. 22, no. 1., 2005.

[12] B. Balaraju1, M. Kuppan, S. H. Babu, S. Kaleemulla, N. M. Rao, C. Krishnamoorthi, G. M. Joshi, G. V. Rao, K. Subbaravamma, I. Omkaram, and D. S. Reddy, "Structural, Optical and Magnetic Properties of α-Fe_2O_3 Nanoparticles3," *MMSE Journal. Open Access*, vol. 9, p. 10.2412, 2017.

[13] D. Samsonov, S. Zhdanov, G. Morfill and V. Steinberg, "Levitation and agglomeration of magnetic grains in a complex (dusty) plasma with magnetic field," *New J. Phys.*, vol. 5, pp. 24.1-24.10, 2003.

[14] M. Rosenberg, D. P. Sheehan and J. R. Petrie, "Use of Dusty Plasmas for Surface-Enhanced Vibrational Spectroscopy Studies," *J. Phys. Chem. A*, vol. 108, no. 26, pp. 5573–5575, 2004.

[15] Y. K. Jabur, M. G. Hammed, and M. K. Khalaf, "DC Glow Discharge Plasma Characteristics in Ar/O2 Gas Mixture," *Iraqi Journal of Science*, vol. 62, no. 2, pp. 475-482, 2021.

[16] T. A. Hameed and S. J. Kadhem, "Plasma diagnostic of gliding arc discharge at atmospheric pressure," *Iraqi Journal of Science*, vol. 60, no. 12, pp.2649-2655, 2019.

[17] H. R. Humud and S. Hussein, "Optical emission spectroscopy for studying the exploding copper wire plasma parameters in distilled water," *Iraqi J. Phys.*, vol. 15, no. 35, pp. 142–147, 2017.

[18] S. S. Hamed, "Spectroscopic Determination of Excitation Premixed Laminar Flame," *Egypt. J. Solids*, vol. 28, no. 2, pp. 349–357, 2005.

[19] N. M. Shaikh, S. Hafeez, B. Rashid, and M. A. Baig, "Spectroscopic studies of laser induced aluminum plasma using fundamental, second and third harmonics of a Nd : YAG laser," *Eur. Phys. Journal D*, vol. 44, pp. 371–379, 2007.

[20] C. Fallon, "Optical Diagnostics of Colliding Laser Produced Plasmas : Towards Next Generation Plasma Light Sources," PhD thesis, Dublin City University, 2013.

[21] N. Konjevic and W. L. Wiese, "Experimental Stark widths and shifts for spectral lines of neutral and ionized atoms," *J. Phys. Chem. Ref. Data*, vol. 19, no. 6, pp. 1307–1385, 1990.